The late Oligocene Cieneguilla basanites, Santa Fe County: Records of early Rio Grande rift magmatism

Jennifer Lindline, Michael Petronis, Rachell Pitrucha, and Salvador Sena, 2011, pp. 235-250

in:

Geology of the Tusas Mountains and Ojo Caliente, Author Koning, Daniel J.; Karlstrom, Karl E.; Kelley, Shari A.; Lueth, Virgil W.; Aby, Scott B., New Mexico Geological Society 62nd Annual Fall Field Conference Guidebook, 418 p.

This page is intentionally left blank to maintain order of facing pages.

THE LATE OLIGOCENE CIENEGUILLA BASANITES, SANTA FE COUNTY: RECORDS OF EARLY RIO GRANDE RIFT MAGMATISM

JENNIFER LINDLINE, MICHAEL PETRONIS, RACHELL PITRUCHA, AND SALVADOR SENA
Environmental Geology Program, New Mexico Highlands University, P.O. Box 9000, Las Vegas, NM 87701, lindlinej@nmhu.edu

ABSTRACT—We conducted petrogenetic studies of 25-26 Ma Cieneguilla basanites of the Cieneguilla volcanic field in the southern Española Basin to improve our understanding of early Rio Grande rift magmatism. We sampled 3-4 lava flows at two different locations north of La Cienega: an unnamed knoll (LCB1) and Cerro Seguro (LCB2). All sampled Cieneguilla basanites are olivine porphyritic, magnetic, slightly vesicular, and relatively unweathered. They contain mildly to moderately altered olivine phenocrysts in a very fine-grained framework of intergranular clinopyroxene-magnetite and interstitial nepheline. The estimated titanium content of the Fe-Ti oxide phase ranges from 0.106-0.210 at LCB1 and from 0.019-0.115 at LCB2. The Cieneguilla basanites are mildly alkaline and fall within the sodic series of the alkali olivine basalt scheme. They have low silica values (42.40-44.10 wt %) and high MgO values (11.50-13.50 wt %) and are some of the most primitive eruptive products in the central Rio Grande rift. The rocks display a narrow range of CaO (10.68-11.45 wt %), $FeO+Fe_2O_3$ (12.37-13.25 wt %), K_2O (0.61-1.05 wt %) and TiO_2 (2.16-2.37 wt %). Compatible trace elements, like Sr (758-1031 ppm), Cr (457-553 ppm), Ni (263-288 ppm), and Co (61.1-67.6 ppm) show a wider range of concentrations. The major and trace element values are sufficiently distinct between LCB1 and LCB2 to suggest that they are separate batches of magma, yet similar trace element patterns suggest that they share a similar source. The basanites are enriched in LREE relative to HREE ($(La/Yb)_N$=18-26). They have $(La/Nb)_N$ values between 1.2-1.5 and moderately high Nb/Ba and Ta/Ba ratios consistent with an origin from an ocean island basalt-modified lithosphere source region. These data suggest that the Cieneguilla basanites have both asthenospheric and lithospheric mantle components and that the Rio Grande rift contained mixed mantle source regions during its early history.

INTRODUCTION

La Cienega, a historic village 30 km southwest of Santa Fe, NM, hosts the Cienega volcanic field (Fig. 1) which comprises several lava flows and monogenetic cones, including Cerro Seguro (Figs. 1-3). The volcanic rocks include basanite, nephelinite, and basalt that overlie or intrude the Tertiary Espinosa Formation (Koning and Read, 2010). They are major localities for the Cieneguilla Limburgite Formation (Stearns, 1953 a, b; Sun and Baldwin, 1958), which was redefined as the Cieneguilla basanite by Koning and Hallett (2000), Sawyer et al. (2002) and Koning and Read (2010). The Cieneguilla basanite is one of the lowermost volcanic units in the La Cienega area. Near La Cienega, the Cieneguilla basanite yielded a K-Ar age determination of 25.1±0.7 Ma (Baldridge et al., 1980) and a $^{40}Ar/^{39}Ar$ age determination of 26.08±0.62 Ma (Peters, 2000; Koning and Hallett, 2000). These values are similar to a K-Ar date of 25.1±0.6 Ma (Kautz et al., 1981) and a $^{40}Ar/^{39}Ar$ date of 25.41±0.32 Ma (Connell et al., 2002) obtained from an olivine tholeiite at Espinaso Ridge west of Cerrillos. The Cieneguilla basanites are significant as these flows erupted before the main episode of Rio Grande rifting (10 to 16 Ma) in northern New Mexico (Keller and Cather, 1994).

We conducted a petrologic study of the Cieneguilla basanite to improve our understanding of early Rio Grande rift magmatic processes. We chose the Cieneguilla basanites because these low volume lava flows have the potential to yield information about mantle source region(s) without the problems of open-system magmatism and/or crustal contamination that have been observed in large-scale volcanism in northern New Mexico (Singer and Kudo, 1986; Duncker et al., 1991; Wolff et al., 2000; Wolff et al., 2005). Previous workers (Stearns 1953 a, b; Sun and Baldwin, 1958) studied the Cieneguilla basanites in the context of broader studies of volcanic rocks of the Cienega area. They reported petrographic features and major element analysis noting the low silica content of the flows. This is the first report of trace and rare earth element geochemistry of the Cieneguilla basanites and the first petrogenetic study of these flows.

GEOLOGY

Setting

The Rio Grande rift is a late Cenozoic continental rift extending south from at least Leadville, Colorado to Chihuahua, Mexico. It represents the easternmost expression of widespread continental extension in the western United States during the past 30 million years. The Rio Grande rift is characterized by normal faulting, basin formation, and predominantly mafic volcanism. The northern part of the rift is relatively narrow, consisting of an array of north-trending westward-stepping, en echelon basins, including the Española Basin, separated by northeast-trending oblique accommodation zones (Rosendahl, 1987; Chapin, 1988) (Fig. 1). The Cienega volcanic field lies at the southern periphery of the intersection of the Rio Grande rift and the Jemez Lineament, an 800-km-long alignment of late Cenozoic volcanic fields (Aldrich 1986). The lineament is considered to be related to a complex suture zone between the Mesoproterozoic Southern Yavapai and the Mazatzal lithospheric provinces (Magnani et al., 2004).

The Cieneguilla basanite volcanoes are located west of the southern Sangre de Cristo Mountains on an elevated structural plateau in the southern Española Basin (Fig. 2) that exposes pre-

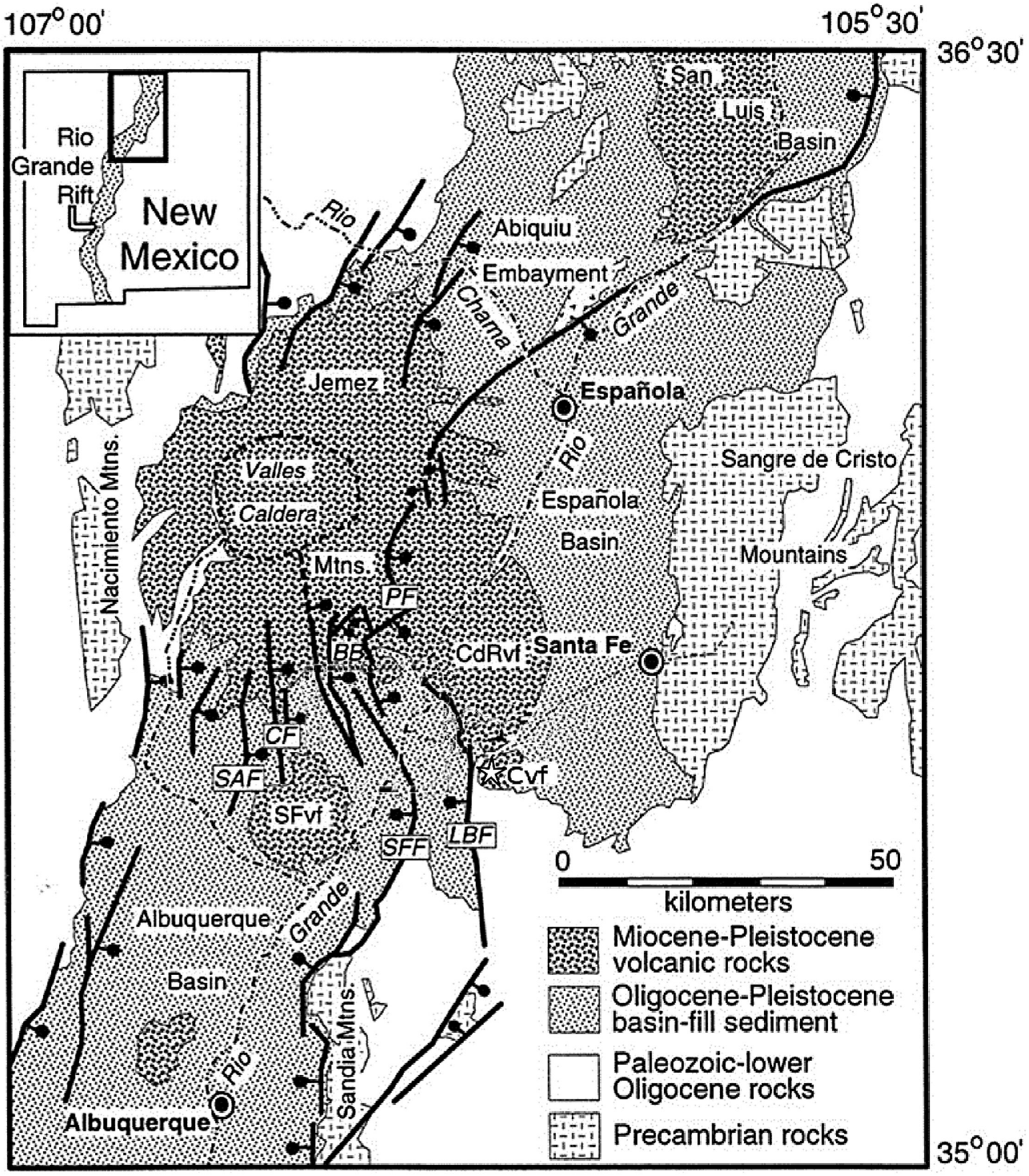

FIGURE 1. Index map of the Rio Grande rift in northern New Mexico showing principal faults, volcanic features, and basins. CF–Cocida fault, LBF–La Bajada fault, PF–Pajarito fault, SAF–Santa Ana fault, SFF–San Francisco fault, BB– Bearhead basin, CdRvf–Cerros del Rio volcanic field, SFvf–San Felipe volcanic field, and Cvf–Cienega volcanic field. Figure modified from Smith et al. (2001).

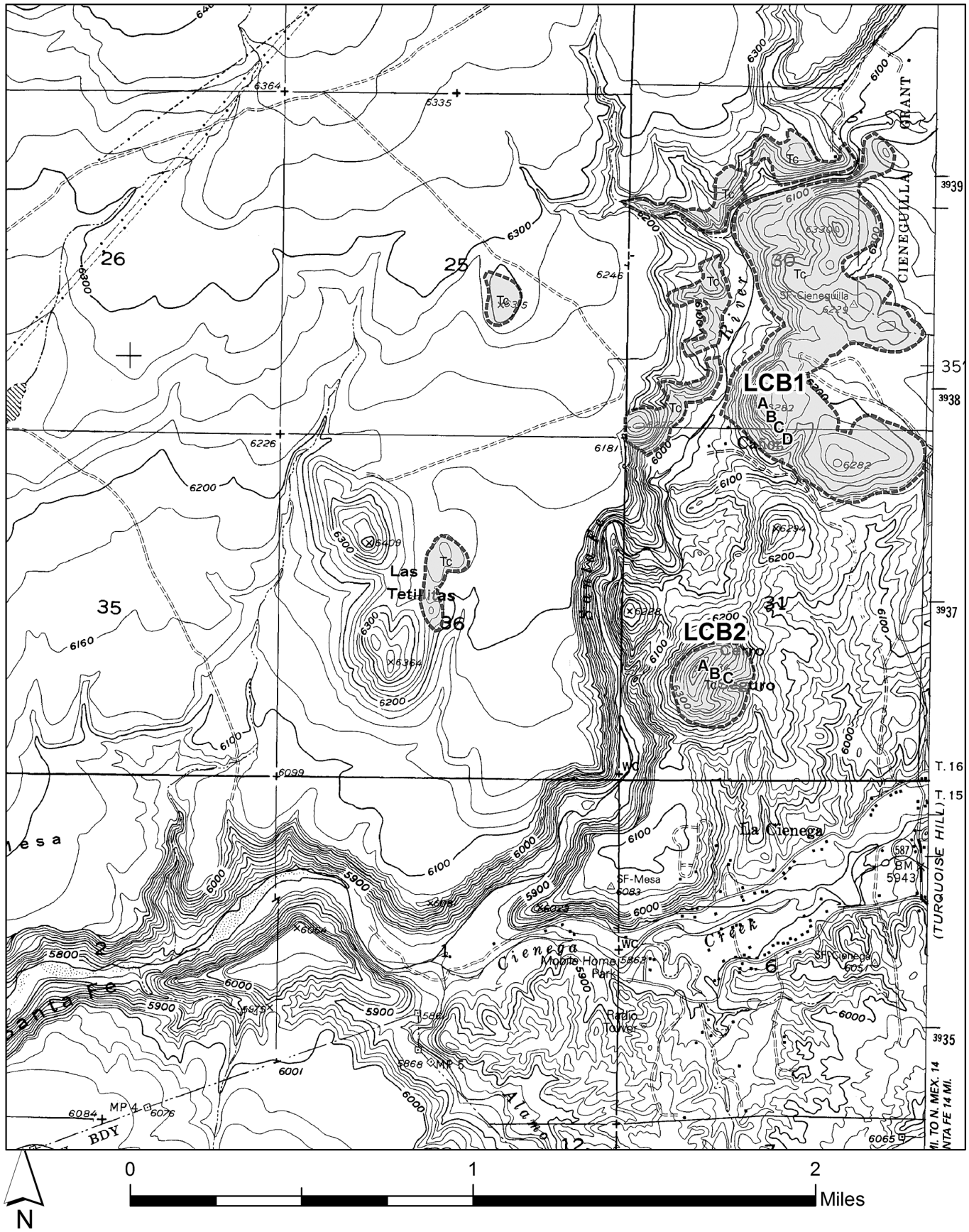

FIGURE 2. Topographic map of the La Cienega area showing the distribution of Cieneguilla basanites (Tc) and sampling localities.

rift and early rift igneous and sedimentary deposits. The area is separated from younger basalt flows of the Cerros del Rio volcanic field to the west by a steep canyon carved by the Santa Fe River as it merges with its main tributary, Cienega Creek, and flows westward toward the Rio Grande. The small volume and somewhat massive Cieneguilla basanite flows erupted through Eocene sedimentary rocks and Tertiary volcanic rocks (Koning and Read, 2010), some of which are related to a north trending chain of volcanic centers of monzonitic-latitic activity that includes the Cerrillos and Ortiz Mountains.

The Cieneguilla basanite crops out on Cerro Seguro and several unnamed hills north and northwest of the historic village of La Cienega (Fig. 3). La Cienega was part of the original La Cieneguilla land grant, which the king of Spain conferred to Francisco de Anaya de Almazán in 1695. The area was an important stopping point (paraje) along the famous Camino Real, the royal road from Mexico City to Santa Fe. Both La Cienega and La Cieneguilla were built over prehistoric pueblos and boast hundreds of petroglyphs dating from pre-contact time and from the Spanish colonial era. The petroglyphs can be found along the Santa Fe River escarpment that includes the Cieneguilla basanites as well as basalts of the younger (2.3-2.8) Cerros del Rio volcanic field (WoldeGabriel et al., 1996).

We sampled the Cieneguilla basanites at two locations: an unnamed hill (LCB1; n=4) and Cerro Seguro (LCB2; n=3) (Fig. 2). We collected samples at several elevations within the individual flow sequences to gain a cross-sectional perspective. At each site, the uppermost flow is noted with the letter A and successively lower flows are noted with the letters B, C, and D respectively. We studied the rocks macroscopically, petrographically, magnetically, and geochemically.

Field Characteristics

The Cieneguilla basanites crop out as small knolls in the Cienega volcanic field. Each hill consists of five or more flows that are a meter or more in thickness. Individual flows dip moderately to the east and are identified by a subtle planar parting parallel to the hill contours and a rubble zone at the base of the fracture planes (Fig. 4). Individual flows can be traced only short distances vertically and laterally because of discontinuous exposures. The basanites are chocolate brown on weathered surfaces and dark black on freshly exposed surfaces. The rocks are very-fine grained, aphyric to slightly porphyritic, and sometimes vesicular. Unlike many basalts in the region, the rocks show little pedogenic carbonate mineralization. All of the flows are strongly magnetic. The flows at LCB1 are unconformably overlain by light-colored unconsolidated sands and gravel of the upper Pliocene to lower Pleistocene Ancha Formation of the Santa Fe Group (Koning and Read, 2010). The Cerro Seguro basanites erupted through a Tertiary (Koning and Read, 2010) augite- and plagioclase-porphyritic felsite intrusion and contain centimeter to decimeter-sized xenoliths of the felsite at lower elevations (Figs. 5 and 6). Basanite at the top of Cerro Seguro shows a monolithic agglomeritic texture and is interpreted as an eruptive center. The agglomerate is approximately 15 m thick and overlies approximately 60 m of dense basaltic lavas.

Petrography

Petrographic analysis of 7 thin sections prepared from each of the sampled Cieneguilla basanite flows was completed using a Meiji Techno 9000-series polarizing microscope. Crystal size was measured using a stage micrometer. Modal mineral analyses

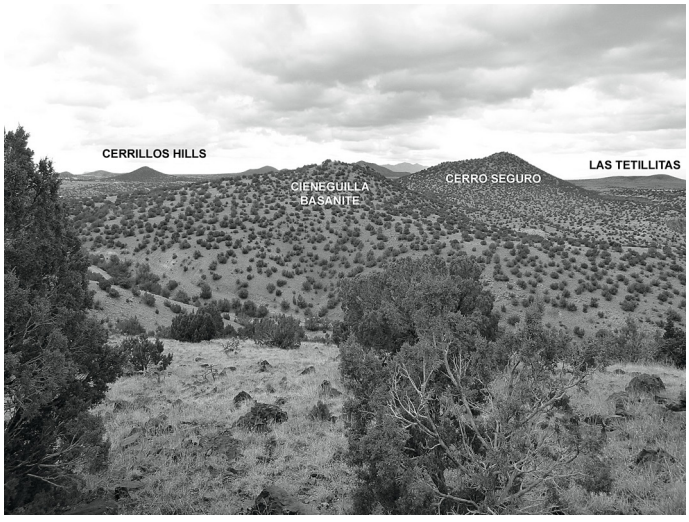

FIGURE 3. View southwest from Cieneguilla basanite site LCB1. Of note are the Cerrillos Hills, which are underlain by the 34-30 Ma Cerrillos Hills Igneous Complex (Maynard, 2005); Las Tetillitas cones of the <3.0 Ma Cerros del Rio volcanic field (WoldeGabriel et al., 1996); and Cerro Seguro and the hill in the foreground, both comprised of 25-26 Ma Cieneguilla basanite.

FIGURE 4. Field photograph of the Cieneguilla basanite at site LCB1-A. Hammer (30 cm length) for scale. The contact between flows is defined by a weak planar parting as well as a rubble zone at the base of each flow.

FIGURE 5. Field photograph of the Cieneguilla basanite at Cerro Seguro, site LCB2-A. Hammer (30 cm length) for scale. Note the agglomeritic texture of the basanite indicating proximity to the vent.

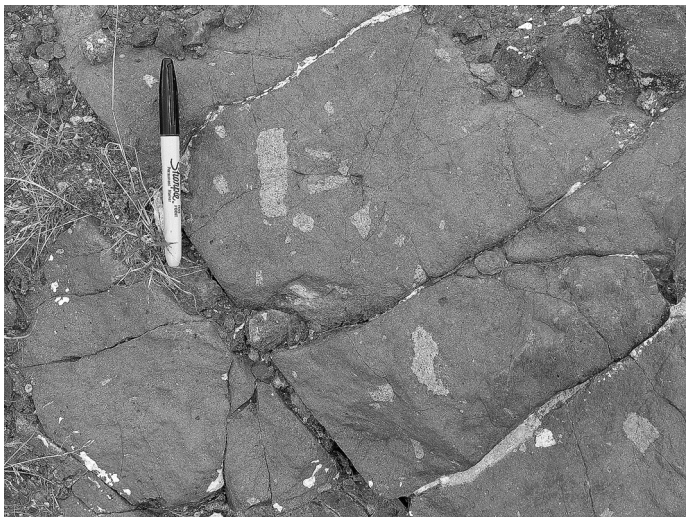

FIGURE 6. Field photograph of the Cieneguilla basanite at Cerro Seguro below site LCB2-C. The marker (10 cm length) is placed for scale. Note the white salt-pepper textured augite- and plagioclase-porphyritic felsite xenoliths throughout the basanite.

of the 7 sections were made using a Priori Scientific Model G automatic point counter set at an interval spacing of 0.25 x 0.25 mm.

The samples are holocrystalline and consist of four primary minerals: olivine, clinopyroxene, magnetite, and nepheline. Modal mineral analysis, based on 1000 point counts, is presented in Table 1. Three repeated analyses of one sample (LCB1-A) indicate that counts are reproducible within 2.45 vol. %. In contrast to the findings of Sun and Baldwin (1958), glass was not present in any of our samples. The samples are porphyritic to partly glomerophyric. Euhedral to subhedral olivine phenocrysts have an average diameter of 0.35 mm with one rare crystal measuring 8.0 mm in length. Olivine phenocrysts make up approximately 25% of the rock with nearly 50% of the phenocrysts being unaltered and the remainder being altered to iddingsite. The groundmass comprises interlocking euhedral clinopyroxene (<0.10-0.70 mm) and magnetite crystals (0.10-0.25 mm) with interstitial and unaltered nepheline. The magnetite crystals display a homogeneous pale gray reflectivity.

Rock Magnetism

We conducted an analysis of the high-temperature low-field magnetic susceptibility on one sample from each of the 7 flows to describe the magnetic character of the Cieneguilla basanites. All susceptibility experiments were measured with an AGICO MFK1-A kappabridge with a CS-4 attachment at the New Mexico Highlands University Paleomagnetism-Rock Magnetism Laboratory. The low-field susceptibility measurements were carried out in a stepwise heating/cooling fashion from 25°C to 700°C to 40°C in an argon atmosphere. Approximately 0.55 g of powdered sample from each lava flow was used in each analysis. The susceptibility experiments allow for an evaluation of the magnetic mineral composition based on Curie point estimates and assist with revealing mixtures of magnetic phases within a given sample. Pure magnetite has a Curie point of ~580°C, which decreases nearly linearly with increasing Ti substitution to

TABLE 1. Cieneguilla basanite modal mineralogy presented as percentages. Modes were calculated based on 1000 point counts.

Replicate analysis of LCB1-A showing reproducibility of counts within 2.45 volume percent.

	LCB1-A1	LCB1-A2	LCB1-A3	AVG	STD DEV
olivine	9.30	12.00	12.90	11.40	1.53
clinopyroxene	46.90	45.60	47.10	46.53	0.66
nepheline	8.10	9.30	9.20	8.87	0.54
magnetite	23.50	20.80	17.50	20.60	2.45
iddingsite	12.20	12.30	13.30	12.60	0.50

Analysis of the individual basanite samples showing variability within the sample set.

	LCB1-A1	LCB1-B	LCB1-C	LCB1-D	LCB2-A	LCB2-B	LCB2-C	AVG	STD DEV
olivine	9.30	10.30	12.60	10.40	12.30	9.90	17.40	12.04	2.38
clinopyroxene	46.90	39.40	47.30	43.70	44.30	34.90	30.90	41.00	5.74
nepheline	8.10	25.00	11.40	17.70	18.20	23.70	29.10	19.14	6.79
magnetite	23.50	10.20	19.40	1.30	13.20	17.30	12.30	13.47	6.11
iddingsite	12.20	15.10	9.30	16.90	12.30	14.20	10.30	12.96	2.47

approximately -150°C for pure ilmenite (Readman and O'Reilly 1972; Nishitani and Kono, 1983; Moskowitz, 1987). Susceptibility experiments, therefore, provide a quantitative means to estimate Fe-Ti oxide mineral composition based on the Curie point when a single magnetic phase is present within the sample (Akimoto, 1962). Reported Curie points of other common minerals include hematite (675°), pyrrhotite (320°), and greigite (~330°C) (Dunlop and Özdemir, 1997). All inferred Curie points were estimated using either the inflection point (Tauxe, 1998) or Hopkinson peak methods (Moskowitz, 1981).

Results from the susceptibility experiments are shown in Fig. 7. In general, the rock magnetic results between the lower, middle, and upper parts of the two sampled lava flow sections vary considerably indicating a strong variation in magnetic mineralogy between individual lava flows and between locations. The samples yield a spectrum of results that vary from near reversible curves with a single Curie point to more complex irreversible curves. On heating, five of the seven samples (LCB1-A, -B, -C, and D and LCB2-C) monotonically increase in susceptibility with a strong spike in susceptibility at the Curie point which we interpret as a Hopkinson peak (Moskowitz, 1981) at 453°C, 517°C, 475°C, 512°C, and 512°C respectively. The remaining two samples (LCB2-A, -B) yield more complex heating curves with a broad roll-over that lacks a strong spike in susceptibility. For these two samples, the Curie point was estimated based on the inflection point method (Tauxe, 1998) with values at 557°C and 571°C respectively. All samples are nonreversible on cooling indicating that a change in the magnetic mineralogy has occurred during the heating experiment. The room temperature susceptibility for all samples yields intensities in the range of 0.001-0.0001 SI, consistent with a ferromagnetic mineral phase (Dunlop and Özdemir, 1997). The Curie point estimates indicate that the ferromagnetic mineral phase is a low- to moderate-Ti titanomagnetite which is typical of unaltered basalts.

The susceptibility on the cooling curve of three flows (LCB1-A, -B, and -D) is less than the room temperature susceptibility which may indicate that the magnetic fraction is being altered by heating resulting in a phase with a lower susceptibility. Hrouda (2003) concluded that the nature of this alteration is difficult to fully characterize, yet these results are typically interpreted to indicate that the magnetic mineral that homogenizes is titanomaghemite (Özdemir and O'Reilly, 1981 and 1982). Moreover, Hrouda (2003) points out that the lower susceptibility during the cooling cycle may result from (1) the inversion of titanomaghemite to titanium-poor magnetite plus ilmenite during heating and/or (2) the reduction of these phases to form titanomagnetite. Alternatively, the lower susceptibility on the cooling may simply be an artifact of the measurement procedure controlled by the oxygen fugacity of the oven.

The susceptibility on the cooling curve of all three flows from Cerro Seguro (LCB2-A, -B, and -C) and one flow from site 1 (LCB1-C) on the cooling curve is greater than the room temperature susceptibility. This behavior often reflects the situation when a new magnetic phase (magnetite) is generated by heating of a less magnetic phase. The nonreversibility of the curves indicates that a mineralogical change occurred during the experiment (Özdemir and O'Reilly, 1981; 1982). The oxidation of the Fe-Ti oxide phase(s) is inhomogeneous, and during the heating experiment the mineral in some fashion "homogenizes" to a more susceptible phase as reflected by the modest increase in susceptibility (e.g., Hrouda et al., 2006). This behavior is often indicative of low-temperature oxidation, a phenomenon which is commonly observed in submarine basalts (Irving, 1970; Marshall and Cox, 1972; Johnson and Atwater, 1977).

Using the equations from Akimoto (1962) and the titanomagnetite solid solution series $Fe_{3-x}Ti_xO_4$ where x=titanium content, we calculated the composition of the Fe-Ti oxide phase within each flow (Table 2). The calculated titanium content (number of ions) of the Fe-Ti oxide phase ranges from 0.106-0.210 at the first flow sequence and from 0.019-0.115 at Cerro Seguro. These values correspond to a low- to moderate-Ti titanomagnetite phase. The titanomagnetite composition varies within each flow sequence as well as between the flow sequences.

Geochemistry

The bulk rock chemistry of 7 Cieneguilla basanite samples was determined by Activation Laboratories, Ltd., Ontario, Canada. Geochemical data are presented in Tables 3 and 4. All major elements are reported in wt. % oxides; all trace elements are reported in ppm. Samples were digested by fusion with $LiBO_2$ then analyzed for major and trace elements by ICP-MS. Quality control standard analyses show an accuracy of ± 0.65 wt. % for SiO_2, ± 0.35 wt. % for Al_2O_3, and ± < 0.20 wt. % for all other major elements. Accuracy is better than 1% for all trace elements, excepting Cu, V, and Sr for which the concentration of the standard was nearly out of range for the analytical technique. Loss on ignition values range from 0.68-1.23 wt. %, which is low to average for reported Rio Grande rift basalts (Maldonado et al., 2006). For graphical analysis of the major element oxides, the chemical data were normalized to a volatile-free basis. Likewise, the cation normative mineralogy was calculated according to the methods of Irvine and Baragar (1971) adjusting the Fe_2O_3/FeO ratio and recalculating the analyses to 100% on a volatile-free basis.

TABLE 2. Calculated titanium content of the Fe-Ti oxide phase in the Cieneguilla basanites.

Sample	Curie point (◦C)	Ti-Composition
LCB1-A	453	0.210
LCB1-B	517	0.106
LCB1-C	475	0.174
LCB1-D	512	0.115
LCB2-A	557	0.042
LCB2-B	571	0.019
LCB2-C	512	0.115

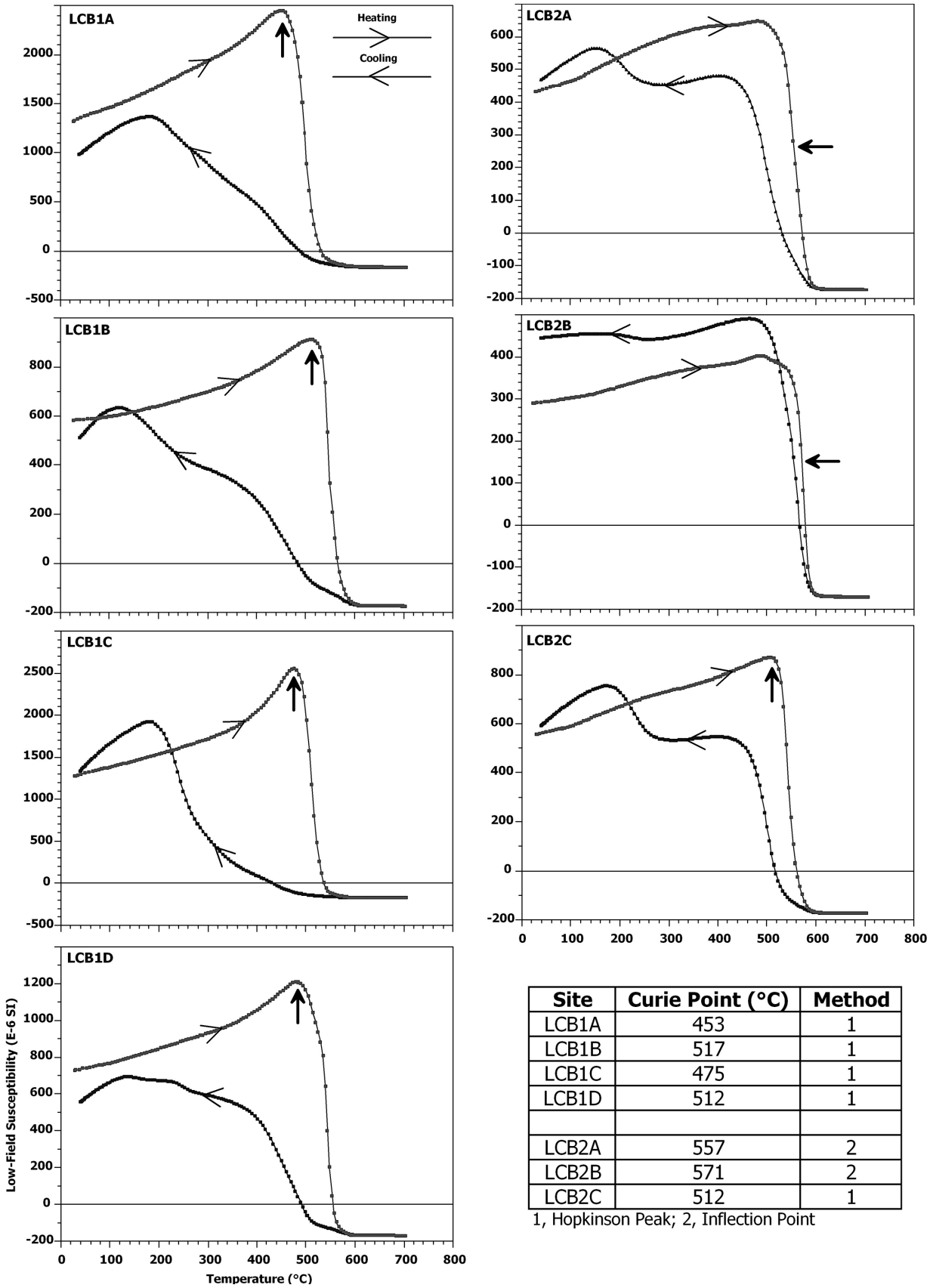

Site	Curie Point (°C)	Method
LCB1A	453	1
LCB1B	517	1
LCB1C	475	1
LCB1D	512	1
LCB2A	557	2
LCB2B	571	2
LCB2C	512	1

1, Hopkinson Peak; 2, Inflection Point

FIGURE 7. Continuous low-field susceptibility vs. temperature experiments from 25°C to 700°C and cooling to 40°C. Results are consistent with the presence of an Fe-Ti oxide phase, likely titanomagnetite. The Ti-content of the titanomagnetite varies within each flow sequence as well as between the two flow sequences.

TABLE 3. Whole rock major element analyses (oxide wt %) and calculated cation normative minerals for the Cieneguilla basanites.

	LCB1-A	LCB1-B	LCB1-C	LCB1-D	LCB2-A	LCB2-B	LCB2-C
[13S] EASTING	0397274	0397274	0397274	0397360	0396926	0396978	0397098
NORTHING	3938018	3937979	3937964	3937946	3936922	3936958	3936887
SiO_2	42.83	44.09	43.60	43.46	42.76	42.40	42.84
Al_2O_3	12.00	12.50	12.47	12.44	12.31	12.04	12.07
FeOmeas	8.11	8.19	8.95	8.41	5.24	6.79	7.29
Fe_2O_3calc	4.89	5.06	4.14	4.67	7.42	5.58	5.16
MnO	0.20	0.20	0.20	0.20	0.21	0.20	0.20
MgO	12.30	11.50	12.10	11.97	11.78	13.25	13.08
CaO	10.84	10.69	10.68	10.89	11.45	11.27	11.25
Na_2O	2.72	2.62	2.72	2.77	2.96	2.92	3.00
K_2O	0.61	0.78	0.76	0.76	1.05	1.02	0.98
TiO_2	2.32	2.19	2.37	2.37	2.19	2.16	2.17
P_2O_5	0.77	0.68	0.76	0.76	0.96	0.90	0.89
CO_2	0.06	0.03	0.10	0.16	0.06	0.09	0.07
H_20+	1.50	1.40	1.50	1.60	1.60	1.60	1.50
H_20-	0.10	0.20	0.20	0.20	0.20	0.20	0.10
TOTAL	99.15	99.93	100.35	100.46	99.98	100.22	100.50
%AN	57.62	55.14	56.83	58.08	66.00	72.12	68.13
or	3.67	4.67	4.52	4.53	6.27	6.04	5.78
ab	14.04	16.53	14.98	14.02	8.96	6.48	7.74
an	19.09	20.32	19.71	19.42	17.40	16.76	16.54
ne	6.50	4.39	5.77	6.63	10.75	11.87	11.48
di	24.46	23.15	22.92	24.03	26.97	26.68	26.68
ol	23.24	22.50	23.09	22.35	20.64	23.45	23.08
mt	4.07	3.91	4.08	4.08	3.90	3.83	3.83
il	3.29	3.09	3.33	3.33	3.08	3.01	3.02
ap	1.64	1.44	1.60	1.60	2.03	1.88	1.86

Note: Total iron was reported as Fe_2O_3. FeO(meas) was measured through titration according to the methods of Wilson (1955). Fe_2O_3(calc) was calculated from the difference between measured total Fe_2O_3 and FeO(meas). CO_2 was determined coulometerically and H_2O+/H_2O- was determined gravimetrically. A 0.3 g sample was thermally decomposed in a resistance furnace in a pure nitrogen environment at 110°C (moisture, H_2O-) followed by decomposition at 1000 °C (interstitial water, H_2O+) using an ELTRA CW-800. Normative mineral abbreviations are as follows: AN=anorthite; or=orthoclase; ab=albite; ne=nepheline; di=diopside; ol=olivine; mt=magnetite; il=ilmenite; and ap=apatite.

All samples show a low and narrow range of silica (42.40-44.09 wt %), though intermediate silica compositions (up to 65.16 wt %) have been noted for volcanic rocks in the Cienega volcanic field (Sun and Baldwin, 1958). The samples are alkaline in composition and part of the sodic series of the alkaline olivine basalt series according to the classification schemes of Irvine and Baragar (1971) (Fig. 8). The samples are silica undersaturated and nepheline normative (4-12% ne). Geochemical variation diagrams are displayed in Figure 9. Samples are plotted against MgO to best differentiate their major oxide and trace element variation. MgO contents of our analyzed samples range from 11.50-13.25 wt %. Across the MgO spectrum, the rocks display a narrow range of CaO (10.68-11.45 wt %), $FeO+Fe_2O_3$ (12.37-13.25 wt %), K_2O (0.61-1.05 wt %) and TiO_2 (2.16-2.37 wt %). Compatible trace elements, like Sr (758-1031 ppm), Cr (457-553 ppm), Ni (263-288 ppm), and Co (61.1-67.6 ppm) show a wider range of concentrations. The major and trace element values are sufficiently distinct between LCB1 and LCB2 to suggest that they are separate batches of magma. LCB1 flows have higher $FeO+Fe_2O_3$, TiO_2, and Co and lower CaO, K_2O, Sr, and Ba than LCB2 flows. However, whether samples from each site are considered separately or as a composite suite, there are no strong trends in major and trace element variations relative to MgO.

Incompatible element and rare earth element (REE) variation plots are shown in Figure 10. The multi-element spectra (Fig. 10a) of these rocks show essentially flat incompatible element patterns between Ba and P, but negative anomalies at K and Sr relative to other trace elements. The basanites are enriched in light rare earth elements (LREE) relative to the heavy rare earth elements (HREE), with $(La/Yb)_N$ ratios varying from 18-26. They have highly incompatible trace element $(La/Nb)_N$ ratios between 1.15-1.32 and low concentrations of large ion lithophile elements (LILE) relative to LREE, with $(Ba/La)_N$ ratios varying from 0.44-0.49.

The tectonic discriminant diagrams FeO-MgO-Al_2O_3 (after Pearce et al., 1977) and Ti/100-Zr-Y*3 diagram (after Pearce and Cann, 1973) were used to compare the geochemistry of the Cieneguilla basanites to the empirically determined geochemistry of rocks from modern-day tectonic environments (Fig. 11). Magma varies in composition depending on its source area; therefore,

TABLE 4. Whole rock trace and rare earth element analyses (ppm) for the Cieneguilla basanites.

	LCB1-A	LCB1-B	LCB1-C	LCB1-D	LCB2-A	LCB2-B	LCB2-C
Ba	619	537	628	618	846	854	858
Co	67.6	64.8	62.8	63.6	62.6	61.8	61.1
Cr	500	457	472	486	549	553	532
Cu	70	78	85	68	67	62	68
Ni	287	263	286	283	284	288	280
Sc	29.6	28.2	28	28.2	29.5	29.6	28.8
Sr	790	758	854	920	1031	990	1030
V	270	272	273	273	269	262	295
Y	23	23	24	25	25	24	25
Zn	94	102	105	100	93	90	91
Cs	1.4	4.7	21.5	46.9	0.6	0.6	0.6
Ga	19	18	19	19	19	18	19
Ge	1.5	1.3	1.5	1.5	1.5	1.5	1.5
Hf	5.9	5.2	5.7	5.7	5.7	5.2	5.9
Nb	54.8	46.4	55.2	55.5	77.7	70.9	79.7
Rb	21	26	26	23	43	43	37
Ta	3.85	3.28	3.66	3.71	4.75	4.58	4.88
Th	11.6	10.4	10.9	10.7	12	11.7	12.2
U	3.05	2	2.43	2.44	2.93	2.85	2.89
Zr	260	228	265	259	274	257	279
La	64.9	57.9	62.4	63.8	85.2	84.2	86.7
Ce	132	115	127	130	167	164	171
Pr	16.2	13.1	15.8	15.9	19.3	19	19.3
Nd	64.1	51.8	62.1	62.1	72.8	71.5	73.9
Sm	11.9	9.53	11.5	11.4	13.1	12.8	13.2
Eu	3.27	2.72	3.25	3.25	3.63	3.55	3.65
Gd	9.69	7.61	9.67	9.32	10.2	9.93	10.2
Tb	1.27	1.05	1.23	1.21	1.33	1.3	1.33
Dy	6.15	5.28	6.09	5.91	6.19	6.16	6.21
Ho	1.1	0.93	1.06	1.06	1.1	1.07	1.11
Er	2.81	2.4	2.76	2.71	2.83	2.72	2.85
Tm	0.366	0.316	0.364	0.352	0.361	0.356	0.369
Yb	2.21	1.97	2.28	2.23	2.22	2.16	2.21
Lu	0.322	0.298	0.323	0.326	0.325	0.317	0.323

analyzing the concentrations of elements that differ with source region makes it possible to determine the source area of igneous extrusive rocks. The FeO-MgO-Al_2O_3 diagram (Fig. 11a) shows that the Cieneguilla basanites have compositions similar to ocean island basalts while the Ti/100-Zr-Y*3 diagram (Fig. 11b) shows that the Cieneguilla basanites have source regions comparable to basalts originating from a within-plate environment.

A number of authors have delineated several chemical types of mantle source for Rio Grande rift mafic volcanism in New Mexico (Perry et al., 1987, 1988; Bradshaw et al., 1993; McMillan, 1998; and McMillan et al., 2000) using trace element and isotopic signatures. The first source region is the convecting asthenosphere, which is isotopically depleted relative to lithospheric reservoirs and has ocean island basalt trace element patterns, particularly high Ta/Ba and high Nb/Ba. The second source region is the lithospheric mantle modified by fluids derived from the convecting asthenosphere (McKenzie, 1989) which produces small degree partial melts under the continents. These fluids impart high Ta/Ba and Nb/Ba and low Ba/La ratios to the lithospheric mantle (McMillan, 1998). The third source region is the lithospheric mantle modified by subduction zone fluids that are rich in fluid-mobilized elements, like Ba, Rb, and Sr. This source region is characterized by high Ba/La and by low Ta/Ba and Nb/Ba as the high field strength elements Ta and Nb are retained in the slab during dehydration and partial melting. Both lithospheric source regions have enriched isotopic signatures (ε_{Nd}~+1 and $^{87}Sr/^{86}Sr$=0.7040-0.7045) that developed over a protracted history as incompatible-rich basaltic magmas and/or metasomatic fluids high in Rb/Sr and Sm/Nd were intruded into the lithosphere and isolated from the underlying convecting asthenosphere. To further evaluate the source region(s) of the Cieneguilla basanites, we compared their trace element compositions to Rio Grande rift source regions. The Cieneguilla basanites have moderately high Nb/Ba and Ta/Ba ratios similar to Rio Grande rift lavas erupted from an ocean island basalt-modified lithosphere source region (Fig. 12).

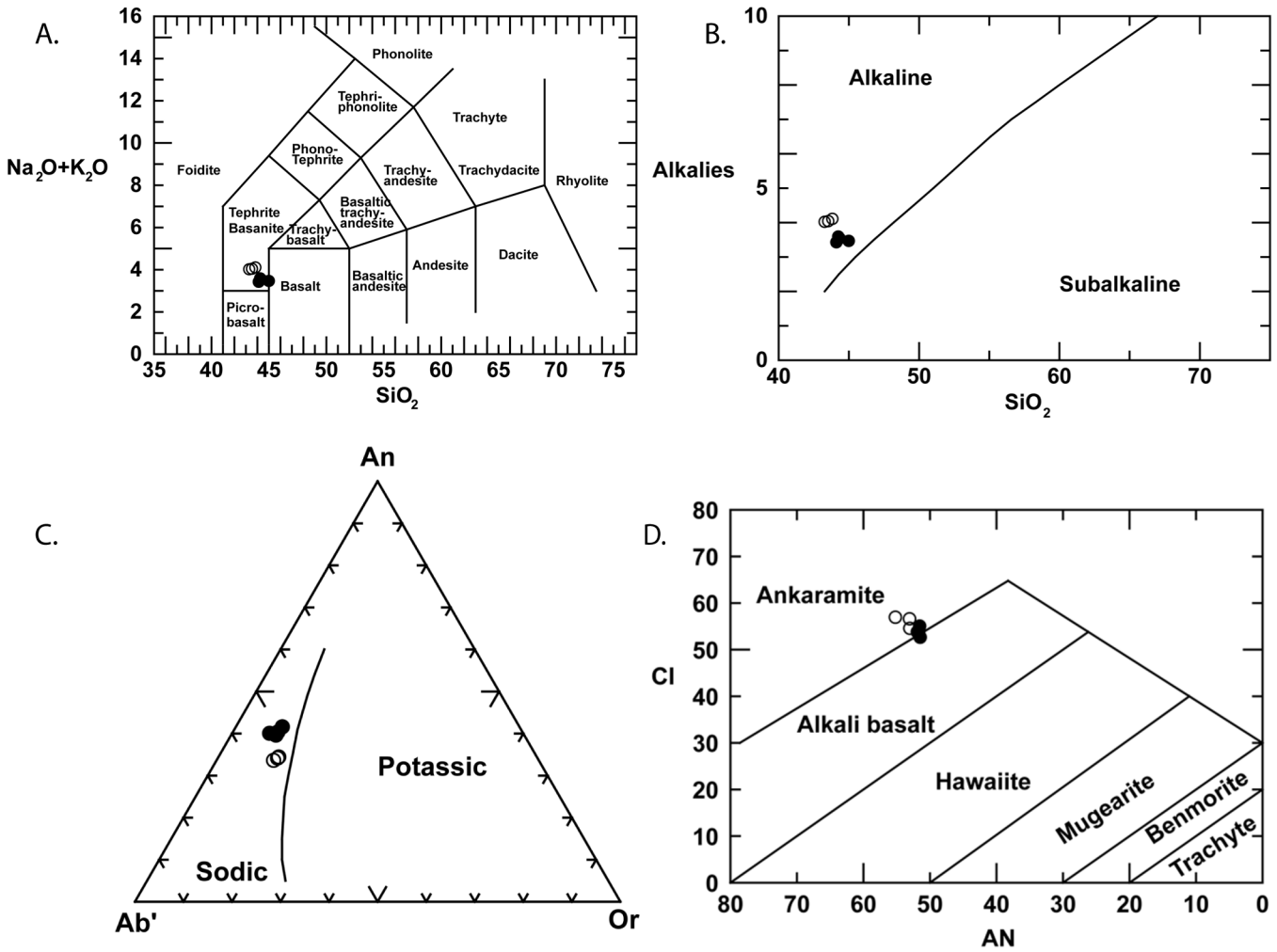

FIGURE 8. Geochemical classification diagrams for the Cieneguilla basanites. Solid circles represent samples from LCB1 and open circle represent samples from LCB2. (A) The samples are basanites according to the IUGS classification scheme (LeBas and Streckeisen, 1991). The samples are (B) alkaline in compositions and (C) part of the sodic series of the (D) alkaline olivine basalt series following the Irvine and Baragar (1971) scheme.

DISCUSSION

The holocrystalline Cieneguilla basanites crystallized phenocrysts of olivine followed by intergranular (titano-)magnetite and clinopyroxene then late interstitial nepheline. The titanomagnetite lacks exsolution textures signifying fast-ascent eruption. The basanites do not show evidence for fractional crystallization, as the modal mineralogy is fairly consistent between the lava flows at each site as well as between the two sites. This is supported by the narrow range of most major oxides as well as the narrow range in most compatible trace elements. The calculated titanium content of the Fe-Ti oxide phase ranges from 0.106-0.210 at the first flow sequence and from 0.019-0.115 at Cerro Seguro. These values indicate that the Cieneguilla basanites contain a low- to moderate-Ti titanomagnetite phase, but that the composition of the titanomagnetite varies between the two studied sites as well as within lava flows from each site. These results could indicate that the magma chamber was evolving quickly between individual eruptions, being replenished by pulses of magma into the chamber following eruption, or undergoing a change in oxygen fugacity. Given the low degree of mineralogical and chemical variation between the lava flows, it is unlikely that the magnetic mineralogy is reflecting differentiation of the magma chamber. Likewise, exsolution lamellae, the degree and scale of which are controlled by variations in cooling rate and oxygen fugacity (Turner et al., 2008), are absent from the titanomagnetite crystals. Thus, it is likely that the variable Ti-content in the titanomagnetite reflects new magma pulses having slightly different bulk rock chemistries. The major and trace element data from the first flow sequence differ from those from Cerro Seguro also implying different magma batches. These batches could have erupted from two discrete magma chambers or there were slight changes in the composition of magma replenishing a single chamber.

Mantle Source Region

The Cieneguilla basanites are mildly alkaline and fall within the sodic series of the alkali olivine basalt scheme. They have low silica values (42.4-44.1 weight percent) and high MgO values

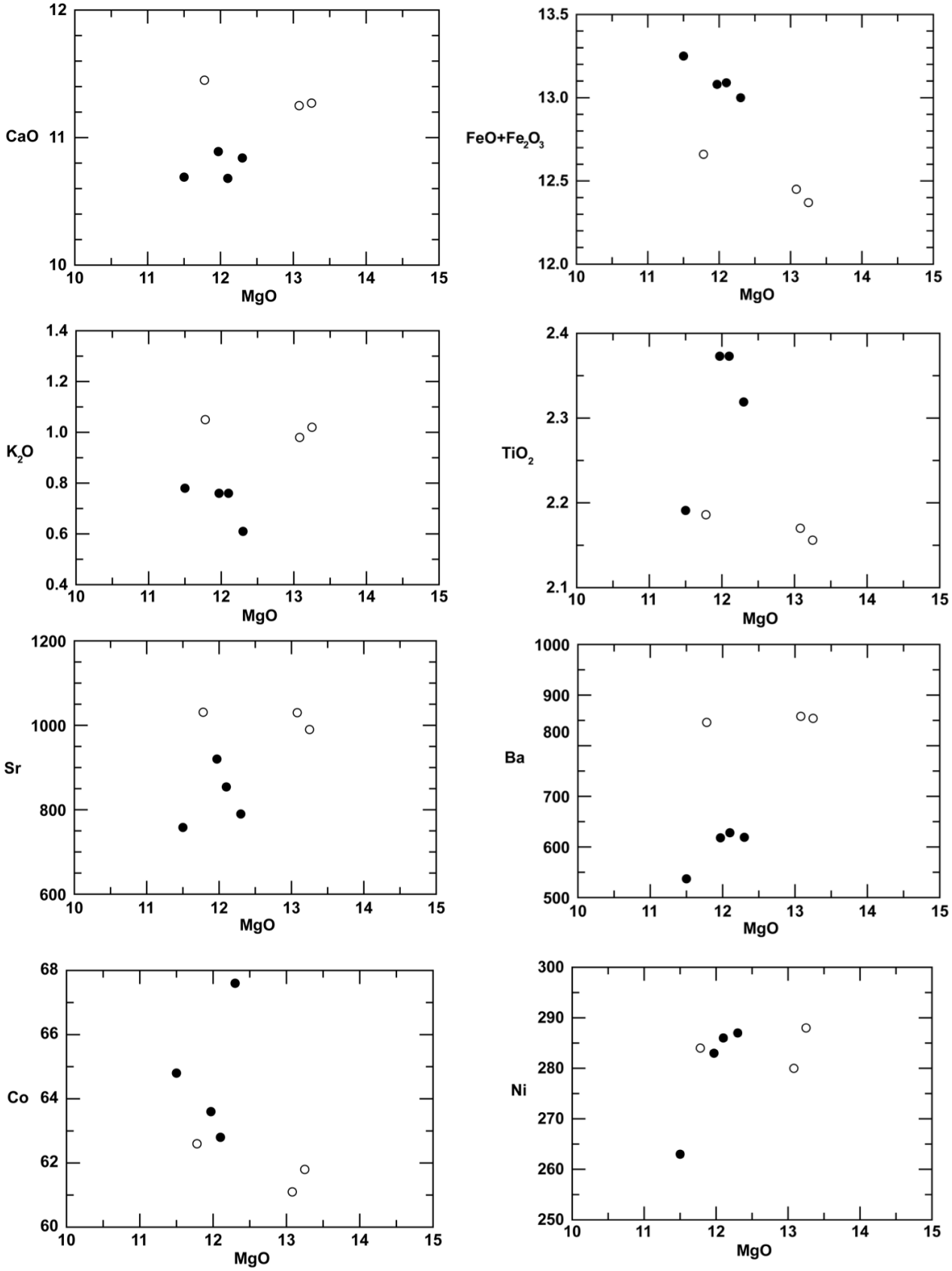

FIGURE 9. Geochemical variation diagrams for the Cieneguilla basanites. All major elements are reported in wt % oxides; all trace elements are reported in ppm. Solid circles represent samples from LCB1 and open circle represent samples from LCB2.

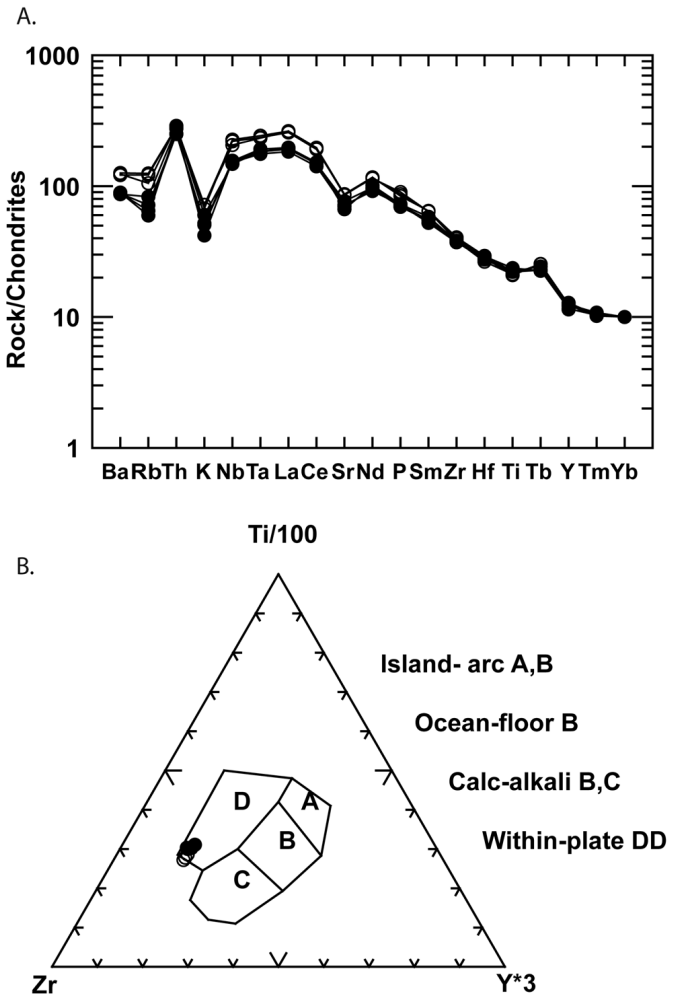

FIGURE 10. (A) Chondrite normalized incompatible element variation and (B) rare earth element variation plots of the Cieneguilla basanites. Solid circles represent samples from LCB1 and open circle represent samples from LCB2. Incompatible element chondrite normalization values are from Thompson et al. (1984). REE chondrite normalization values are from Nakamura (1974).

(11.5-13.5 weight percent) and are some of the most primitive eruptive products in the central Rio Grande rift. The Cieneguilla basanites are sufficiently mafic that their incompatible trace element compositions are controlled mainly by their mantle source region(s). Despite the presence of felsite xenoliths in the Cerro Seguro flows, there does not seem to be any geochemical indication of assimilation or contamination by a crustal component. In fact, the Cerro Seguro flows have the most primitive compositions of the samples collected for this study.

The Cieneguilla basanites are enriched in highly incompatible trace elements (LREE), large ion lithophile elements (Ba, Rb, and K), and high field strength elements (Th and Ta) relative to chondrite (Fig. 10) indicating an undepleted (primitive) and/or enriched mantle source. The basanites are enriched in the LREE relative to the HREE $(La/Yb)_N$=18-26. Chondrite-normalized trace element patterns show a strong enrichment in most incompatible elements, but marked depletions in K and Rb relative to light rare earth elements, Nb, Ta, and Th. These are characteristics of strongly silica-undersaturated ocean island basalts. The basanites have $(La/Nb)_N$ values 1.2-1.5, which are also characteristic of ocean island basalts (Gibson et al., 1991). The K-trough on the multi-element spectra is a characteristic feature of many small-degree partial melts that may denote the incomplete resorption of potassic amphibole or phlogopite in the mantle source (Fitton and Dunlop, 1985).

While both the asthenospheric and lithospheric mantle contributed to mafic magmatism throughout the Rio Grande rift, central Rio Grande rift mafic magmatism, which includes volcanic fields extending from Socorro, New Mexico, to Leadville, Colorado, has been largely attributed to subduction-modified lithospheric mantle which formed from reservoirs established during Proterozoic craton development and affected by slab fluids (McMillan, 1998; Baldridge, 2004). Some Española Basin volcanic rocks having high Ta/Ba and Nb/Ba ratios were interpreted as asthe-

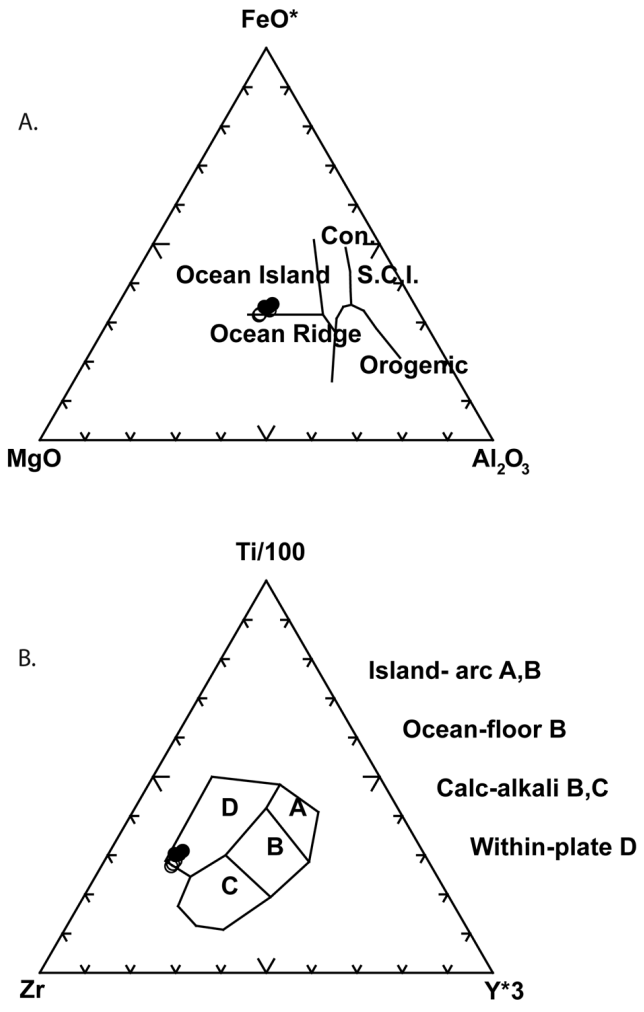

FIGURE 11. Tectonic discrimination diagrams after (A) Pearce et al. (1977) and (B) Pearce and Cann (1973). Solid circles represent samples from LCB1 and open circle represent samples from LCB2. The Cieneguilla basanites plot in the "ocean island" and "within-plate" fields.

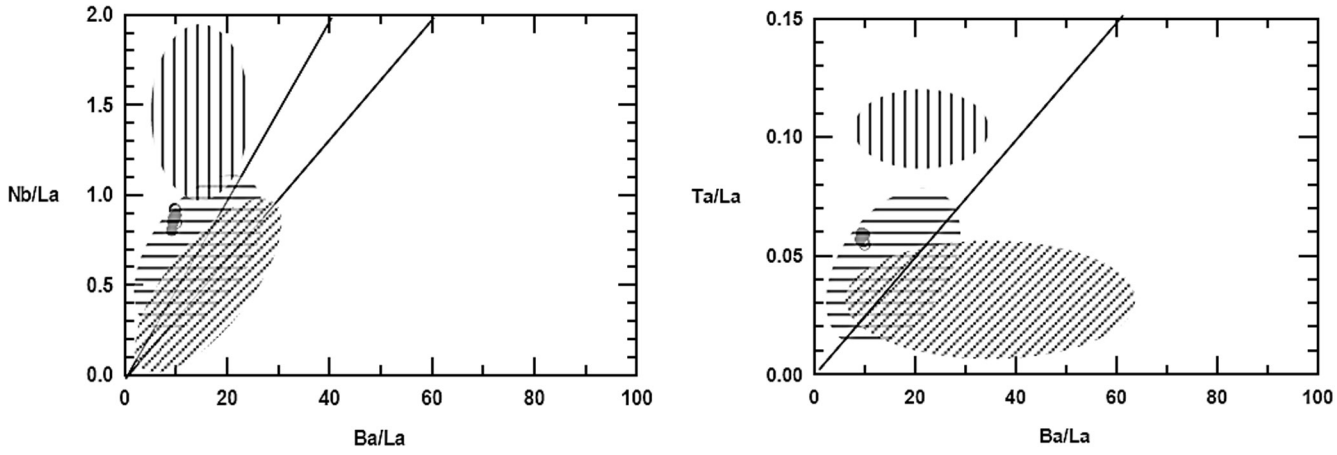

FIGURE 12. Trace element diagrams for the Cieneguilla basanites comparing the compositions of the Cieneguilla basanites to delineated source regions for Rio Grande rift mafic lavas. The vertical-lined area shows the region of asthenospheric source; the horizontal-lined area shows the region of ocean island basalt-modified lithospheric source; and the diagonal-lined area shows the region of subduction-modified lithospheric source (McMillan, 1998). The moderately high Nb/Ba and moderately high Ta/Ba ratios for the Cieneguilla basanites are similar to Rio Grande rift lavas originating from an ocean island basalt-modified lithospheric source.

nospheric melts by Gibson et al. (1992, 1993). McMillan (1998) rejected this notion based on some rocks plotting outside of the modern ocean island basalt fields on tectonic discriminant diagrams and isotopic values that are different and wider ranging than those ascribed to the Oligocene asthenosphere. Rather, the Española Basin volcanic rocks were interpreted as partial melts of an ocean island basalt-modified lithosphere. The plotting of the studied Cieneguilla basanites on tectonic discriminant diagrams (Fig. 11) indicates that the source for the basanites was a within plate ocean island mantle-like reservoir. The moderately high Ta/Ba and moderately high Nb/Ba ratios are indicative of an ocean island basalt-modified lithospheric mantle source, which is consistent with McMillan's (1998) interpretation for ≤ 26 Ma volcanic rocks from the southern Española Basin. Thus, the Cieneguilla basanites have a mixed asthenospheric and lithospheric mantle source. Crow et al. (2011) proposed a model for progressive infiltration and replacement of lithospheric mantle by asthenospheric mantle in the Colorado Plateau during the Neogene where Proterozoic boundaries, like the Jemez lineament, exist. Our data suggest that modification of lithosphere by upwelling asthenosphere created mixed mantle source regions during the early (pre-Neogene) development of the Rio Grande rift.

CONCLUSIONS

Based on the data presented in this study, we conclude the following:

1) The Cieneguilla basanites are some of the most primitive eruptive products in the Cienega volcanic field in particular and the Rio Grande rift in general. They display a low and narrow range of silica (42.40-44.09 wt %) and narrow and high range of MgO (1.50-13.25 wt %).

2) The Ti-content in the titanomagnetite varies between 0.106-0.210 at the first flow sequence and from 0.019-0.115 at Cerro Seguro suggesting that different batches of magma erupted from discrete magma chambers at each site, or that there were slight changes in the composition of magma replenishing a single chamber.

3) Major and trace element values from the first flow sequence differ from those from Cerro Seguro again suggesting that each site represents different batches of magma.

4) The Cieneguilla basanites have trace element characteristics, including $(La/Yb)_N$ values between 18-26, $(La/Nb)_N$ values between 1.2-1.5, and moderately high Ta/Ba and Nb/Ba ratios, that correspond to an ocean island basalt-modified lithosphere source region. This implies that the Cieneguilla basanites have both asthenospheric and lithospheric mantle components.

5) The Rio Grande rift contained mixed mantle source regions during its early (pre-Neogene) history.

ACKNOWLEDGMENTS

We thank Dan Koning for introducing us to the Cieneguilla basanites. The NMHU Office of Research and Sponsored Programs funded geochemical analyses of the Cieneguilla basanites. The NSF-WAESO program provided stipends to support student involvement in this research. David Broxton, Karl Karlstrom, and Giday WoldeGabriel reviewed the manuscript and provided constructive comments.

REFERENCES

Aldrich, M.J., Jr., 1986, Tectonics of the Jemez Lineament in the Jemez Mountains and Rio Grande Rift: Journal of Geophysical Research, v. 91, no. B2, p. 1753-1762.

Akimoto, S., 1962, Magnetic properties of FeO-Fe_2Oa-Ti0_2 system as a basis of rock magnetism: Journal of the Physical Society of Japan, v. 17, Supplement BI, p. 706.

Baldridge, W.S., 2004, Pliocene-Quaternary volcanism in New Mexico and a model for genesis of magmas in continental extension, *in* Mack, G. H. and Giles, K.A., eds., The Geology of New Mexico: A Geologic History, New Mexico Geological Society, Special Publication 11, p. 312-330.

Baldridge, W.S., Damon, P.E., Shafiqullah, M. and Bridwell, R.J., 1980, Evolution of the central Rio Grande rift, New Mexico: new potassium-argon ages: Earth and Planetary Science Letters, v. 51, p. 309-321.

Bradshaw, T.K., Hawkesworth, C.J., and Gallagher, K., 1993, Basaltic volcanism in the southern Basin and Range: no role for a mantle plume: Earth and Planetary Science Letters, v. 116, p. 45-62.

Chapin, C.E., 1988, Axial basins of the northern and central Rio Grande rifts, *in* Sloss, L. L., ed., Sedimentary Cover-North American craton: US.; the Geology of North America v. D-2, Boulder, Colorado, Geological Society of America, p. 165-170.

Connell, S.D., Cather, S.M., Dunbar, N.W., McIntosh, W.C., and Peters, L., 2002, Stratigraphy of the Tanos and Blackshare Formations (lower Santa Fe Group), Hagan embayment, Rio Grande rift, New Mexico: New Mexico: Geology, v. 24, no. 4, 107-120 p.

Crow, R., Karlstrom, K., Asmerom, Y., Schmandt, B., Polyak, V. and DuFrane, S.A., 2011, Shrinking of the Colorado Plateau via lithospheric mantle erosion: Evidence from Nd and Sr isotopes and geochronology of Neogene basalts: Geology, v. 39, p. 27-30.

Dunker, K.E., Wolff, J.A, Harmon, R.S., Leat, P.T., Dickin, A.P. and Thompson, R.N., 1991, Diverse mantle and crustal components in lavas of the NW Cerros del Rio volcanic field, Rio Grande rift, New Mexico: Contributions to Mineralogy and Petrology, v. 108, p. 331-345.

Dunlop, D.J. and Özdemir, O., 1997, Rock magnetism: fundamentals and frontiers: United Kingdom, Cambridge University Press, 573 p.

Fitton, J.G. and Dunlop, H.M., 1985, The Cameroon Line, West Africa, and its bearing on the origin of oceanic and continental alkali basalts: Earth and Planetary Science Letters, v. 72, p. 23-38.

Gibson, S.A., Thompson, R.N., Leat, P.T., Morrison, M.A., Hendry, G.L., and Dickin, A.P., 1991, The Flat Top volcanic field 1. Lower Miocene open-system, multisource magmatism at Flanker, Trappers Lake: Journal of Geophysical Research, v. 96, p. 13,609-13,267.

Gibson, S.A., Thompson, R.N., Leat, P.T., Dickin, A.P., Morrison, M.A., Hendry, G.L., and Mitchell, J., 1992**,** Asthenosphere-derived magmatism in the Rio Grande rift, western USA: implications for continental break-up, in Storey, B.C., Alabaster, T. And Pankhurst, R.J., eds., Magmatism and the causes of continental break-up, Geological Society of London, Special Publications 68, p. 61-89;

Gibson, S.A., Thompson, R.N., Leat, P.T., Morrison, M.A., Hendry, G.L., Dickin, A.P., and Mitchell, J.G., 1993, Ultrapotassic magmas along the flanks of the Oligo-Miocene Rio Grande Rift, USA: monitors of the zone of lithospheric mantle extension and thinning beneath a continental rift: Journal of Petrology, v. 34, p. 187-228.

Hrouda F., 2003, Indices for numerical characterization of the alteration processes of magnetic minerals taking place during investigation of temperature variation of magnetic susceptibility: Studia Geophysica et Geodaetica, v. 47, p. 847−861.

Hrouda, F., M. Chlupacova, and S. Mrazova, 2006, Low-field variation of magnetic susceptibility as a tool for magnetic mineralogy of rocks: Physics of the Earth and Planetary Interiors, v. 154, no. 3-4, p. 323–336, doi:10.1016/j.pepi.2005.09.013.

Irvine, T.N. and Baragar, W.R.A. 1971, A guide to the chemical classification of the common volcanic rocks: Canadian Journal of Earth Sciences, v. 8, p. 523-548.

Irving, E., 1970, The Mid-Atlantic Ridge at 45°N. XIV. Oxidation and magnetic properties of basalt; review and discussion: Canadian Journal of Earth Sciences, v. 7, p. 1528-1538.

Johnson, H. P. and T. Atwater, 1977, A magnetic study of the basalts from the Mid-Atlantic Ridge at 37°N: Geological Society of America Bulletin, v. 88, 637–647 p.

Kautz, P.F., Ingersoll, R.V., Baldridge, W.S., Damon, P.E. and Shafiqullah, M., 1981, Geology of the Espanaso Formation (Oligocene), north-central New Mexico: Summary: Geological Society of America Bulletin, v. 92, p. 980-983.

Keller, G.R. and Cather, S.M., 1994, Basins of the Rio Grande rift: Structure, stratigraphy, and tectonic setting: Geological Society of America Special Paper 291, 304 p.

Koning, D.J. and Read, A.S., 2010, Geologic Map of the Southern Española Basin, New Mexico Bureau of Geology and Mineral Resources Open File Report 531, scale 1:48,000.

Koning, D.J. and Hallett, R.B., 2000, Geology of the Turquoise Hill 7.5-minute quadrangle, Santa Fe County, New Mexico: New Mexico Bureau of Mines and Mineral Resources, Open-file Geologic Map OF-GM 41, scale 1:24,000.

LeBas, M.H. and Streckeisen, A.L., 1991, The IUGS systematic of igneous rocks: Journal of Geological Society of London, v. 148, p. 825-833.

Maldonado, F., Budahn, J.R., Peters, L., and Unruh, D.M., 2006, Geology, geochronology, and geochemistry of basaltic flows of the Cat Hills, Cat Mesa, Wind Mesa, Cerro Verde, and Mesita Negra, central New Mexico: Canadian Journal of Earth Sciences, v. 43, no., 9, p. 1251–1268 (2006), doi:10.1139/E06-018.

Magnani, M.B., Miller, K.C., Levander, A., and Karlstrom, K., 2004, The Yavapai-Mazatzal boundary: A long-lived tectonic element in the lithosphere of southwestern North America: Geological Society of America Bulletin, v. 116, p. 1137-1142.

Marshall, M. and Cox, A, 1972, Magnetic changes in pillow basalts due to sea floor weathering: Geophysical Research, v. 77, p. 6459-6469.

Maynard, S., 2005, Laccoliths of the Ortiz porphyry belt, Santa Fe County, NM, New Mexico: Geology, v. 27, no. 1, p. 3-21.

McKenzie, D., 1989, Some remarks on the movement of small melt fractions in the mantle: Earth and Planetary science Letters, v. 95, p. 53-72.

McMillan, J.J., 1998, Temporal and spatial magmatic evolution of the Rio Grande Rift: N.M. Geological Society, 49th Field Conference Guidebook, p. 107-116.

McMillan, N.J, Dicken, A.P., and Haag, D., 2000, Evolution of magma source regions in the Rio Grande rift, southern New Mexico: Geological Society of America Bulletin, v. 112, p. 1582-1593.

Moskowitz, B. M., 1981. Methods of estimating Curie temperatures of titanomagnetites from experimental Js-T data: Earth and Planetary Science Letters, v. 53, p. 84-88.

Moskowitz, B. M., 1987, Towards resolving the inconsistencies in characteristic physical properties of synthetic titanomaghemite: Physics of the Earth and Planetary Interiors, v. 46, 173–183, doi:10.1016/0031-9201(87)90180-4.

Nakamura, N. 1974, Determination of REE, Ba, Fe, Mg, Na, and K in carbonaceous and ordinary chondrites: Geochimica et Cosmochemica Acta, 38: 757-775.

Nishitani, T. and M. Kono, 1983, Curie temperature and lattice constant of oxidized titanomagnetite: Geophysical Journal Royal Astronomical Society, v. 74, p. 585–600.

Özdemir, O. and O'Reilly, W., 1981, High-temperature hysteresis and other magnetic properties of synthetic monodomain titanomagnetites: Physics of the Earth and Planetary Interiors, v. 25, p. 406– 418, doi:10.1016/0031-9201(81)90052-2.

Özdemir, O. and W. O'Reilly, 1982, Magnetic hysteresis properties of synthetic monodomain titanomaghemites: Journal of Geomagnetism and Geoelectricity, v. 34, p. 467–478.

Pearce, T. H., Gorman, B. E., Birkett, 1977, The relationship between major element chemistry and tectonic environment of basic and intermediate volcanic rocks: Earth and Planetary Science Letters, v. 36, p. 121-132.

Pearce, J.A. and Cann, J.R., 1973, Tectonic setting of basic volcanic rocks determined using trace element analyses: Earth and Planetary Science Letters, v. 19, p. 290-300.

Perry, F.V., Baldridge, W.S., and DePaolo, D.J., 1987, Role of asthenosphere and lithosphere in the genesis of late Cenozoic basaltic rocks from the Rio Grande rift and adjacent regions of the southwestern United States: Journal of Geophysical Research, v. 92, p. 9193-9213.

Perry, F.V., Baldridge, W.S., and DePaolo, D.J., 1988, Chemical and isotopic evidence for lithospheric thinning beneath the Rio Grande rift: Nature, v. 332, p. 432-434.

Peters, L., 2000, $^{40}Ar/^{39}Ar$ geochronology results from the Cieneguilla basanites, New Mexico Geochronological Research Laboratory, Internal Report, NMGRL-IR-121, 3 p.

Readman, P.W. and O'Reilly, W., 1972, Magnetic properties of oxidized (cation deficient) titanomagnetite (Fe, Ti, $\alpha)_3O_4$: Journal of Geomagnetism and Geoelectricity, v. 24, p. 69-90.

Rosendahl, B. R., 1987, Architecture of continental rifts with special reference to east Africa: Annual Review of Earth and Planetary Science, v. 15, p. 445-503.

Sawyer, D. A., Shroba, R. R., Minor, S. A., and Thompson, R. A., 2002, Geologic map of the Tetilla Peak quadrangle, Santa Fe and Sandoval Counties, New Mexico: U. S. Geological Survey Miscellaneous Field Studies Map MF-2352, scale 1:24,000, version 1.0.

Singer, B.S. and Kudo, A.M., 1986, Assimilation-fractional crystallization of Polvadera Group rocks in the northwestern Jemez Volcanic Field, New Mexico: Contributions to Mineralogy and Petrology, v. 94, p. 374-386.

Smith, G.A., McIntosh, W., and Kuhle, A.J., 2001, Sedimentologioc and geomorphic evidence for seesaw subsidence of the Santo Domingo accommodation-zone basin, Rio Grande rift, New Mexico: Geological Society of America Bulletin, v. 113, no. 5, 561-574 p.

Stearns, C.E., 1953a, Tertiary geology of the Galisteo-Tonque area, New Mexico: Geological Society of America Bulletin 64, 459-508 p.

Stearns, C.E., 1953b, Early Tertiary vulcanism in the Galisteo-Tonque area, north-central New Mexico: American Journal of Science, v. 251, p. 415-452.

Sun, M.S. and Baldwin, B., 1958, Volcanic Rocks of the Cienega Area, Santa Fe County, New Mexico: New Mexico Bureau of Mines and Mineral Resources, Bulletin 54, 80 p.

Tauxe, L., 1998, Paleomagnetic Principles and Practice, v. 17 of Modern Approaches in Geophysics: Dordrecht, Boston, London, Kluwer Academic Publishers.

Thompson, R.N., Morrison, M.A., Hendry, G.L., and Parry, S.J., 1984, An assessment of the relative role of crust and mantle in magma genesis: An elemental approach: Philosophical Transactions of the Royal Society of London, v. A310, p. 549-590.

Turner, M.B. and Cronin, S.J., 2008, Using titanomagnetite textures to elucidate volcanic eruption histories: Geology, v. 36, p. 31-34.

WoldeGabriel, G., Laughlin, A. William, Dethier, D. P., and Heizler, M., 1996, Temporal and geochemical trends of lavas in White Rock Canyon and the Pajarito Plateau, Jemez volcanic field, New Mexico, USA: N.M. Geological Society, 47th Field Conference Guidebook, p. 251-261.

Wolff, J.A., Rowe, M.C., Teasdale, R., Gardner, J.N., Ramos, F.C., and Heikoop, C.E., 2005, Petrogenesis of pre-caldera mafic lavas, Jemez Mountains Volcanic Field (New Mexico, USA): Journal of Petrology, v. 46, p. 407-439.

Wolff, J.A., Heikoop, C.E. and Ellisor, R., 2000, Hybrid origin of Rio Grande rift hawaiites: Geology, v. 28, p. 203-206.

Wilson, A.D., 1955, A new method for the determination of ferrous iron in rocks and minerals: Bulletin of the Geological Survey of Great Britain, v. 9, p. 56-68.